

Inclusion Complexes of Cyclodextrins with Benzoquinolines in Aqueous Solution

Sanyo Hamai

Department of Chemistry, Faculty of Education and Human Studies, Akita University, 1-1 Tegata Gakuen-machi, Akita 010-8502

Received October 24, 2005; E-mail: hamai@ipc.akita-u.ac.jp

The inclusion behavior of cyclodextrins (CDs) towards neutral species of benzo[*h*]quinoline (BhQ), benzo[*f*]quinoline (BfQ), and phenanthridine (PT) have been investigated in pH 7.3 buffers. α-CD forms little or no inclusion complexes with BhQ, BfQ, and PT, whereas β-CD forms 1:1 inclusion complexes with these benzoquinolines. In β-CD solution containing propylene oxide or tetrahydrofuran, a ternary inclusion complex is formed among β-CD, the benzoquinoline, and propylene oxide (tetrahydrofuran). γ-CD forms 1:1 inclusion complexes with the benzoquinolines, except for BhQ, for which a precipitation has been observed in the concentration range examined. For BfQ, its excimer fluorescence has also been observed, which is due to the 2:2 γ-CD–BfQ inclusion complex. The equilibrium constants for the formation of the binary and ternary inclusion complexes have been evaluated from the fluorescence intensity changes.

The inclusion complexation of cyclodextrins (CDs) has been investigated for aromatic hydrocarbons and their derivatives.[1–8] For heterocyclic compounds, on the other hand, there are several studies on the inclusion behavior of CDs; the formation of inclusion complexes of CDs has been examined for acridine, 3*H*-indole, benzo[*a*]phenothiazine, benzothiazoles, dibenzofuran, and so on.[9–14] Because the CD cavity is relatively hydrophobic, a hydrophobic molecule is readily incorporated into the CD cavity when the molecular dimensions of a guest molecule are appropriate to the size of the CD cavity. Due to the hydrophobic cavity of CD, the binding force between CD and a hydrophilic molecule is usually not as strong as that between CD and a hydrophobic molecule. Consequently, a heterocyclic molecule containing a nitrogen atom, which is more hydrophilic than the parent aromatic hydrocarbon molecule, is expected to be bound to the CD cavity to a lesser extent compared to the parent aromatic hydrocarbon.

In heterocyclic molecules containing a nitrogen atom, its substitution position may affect the interactions of the molecules with a CD molecule. Benzo[*h*]quinoline (BhQ), benzo[*f*]quinoline (BfQ), and phenanthridine (PT) are structural analogues, which have a single nitrogen atom substituted for a carbon atom in a phenanthrene skeleton. Although the benzoquinolines contain a nitrogen atom, the solubility in water is relatively low, because the solubility of the parent phenanthrene is very low. In BhQ and BfQ, a pyridine ring is fused to a naphthalene ring, which is readily incorporated into the CD cavity, especially into the β-CD cavity. Consequently, these compounds are expected to be bound to the CD cavity, although the pyridine ring fused to the naphthalene ring somewhat obstructs and/or affects the incorporation of the naphthalene-ring moiety into the CD cavity. Thus, we have investigated the inclusion complexation of CDs with BhQ, BfQ, and PT by means of absorption and fluorescence spectroscopy.

Experimental

BhQ, BfQ, and PT, which were purchased from Tokyo Kasei Kogyo Co., Ltd., were recrystallized from hexane (Scheme 1). β-CD, obtained from Nacalai Tesque, Inc., was recrystallized twice from water, while α-CD and γ-CD, which were obtained from Nacalai Tesque, Inc. and Wako Pure Chemical Industries, Ltd., respectively, were used without further purification. Propylene oxide (PO) and tetrahydrofuran (THF), which were purchased from Wako Pure Chemical Industries, Ltd., were used as received. Buffers (6.7×10^{-4} mol dm^{-3} of KH_2PO_4 and 2.7×10^{-3} mol dm^{-3} of Na_2HPO_4) of pH 7.3 were used throughout this work, except for the experiments of titration. Aqueous solutions of BhQ, BfQ, and PT, which were used for the preparation of sample solutions, were respectively prepared by allowing their purified crystals to be submerged in water for a few days. The concentrations of BhQ, BfQ, and PT in aqueous solutions were calculated under the assumption that, at an absorption peak, their molar absorption coefficients in water are the same as those in methanol.

Absorption spectra were recorded on a Shimadzu UV-2450 UV–vis spectrophotometer. Fluorescence spectra were taken with a Shimadzu RF-501 spectrofluorometer equipped with a cooled Hamamatsu R-943 photomultiplier. The fluorescence spectra were corrected for the spectral response of the fluorometer. Spectroscopic measurements were made at 25 ± 0.1 °C.

The Mulliken charges were calculated with MOPAC using Chem3D Ultra software (CambridgeSoft Corp.).

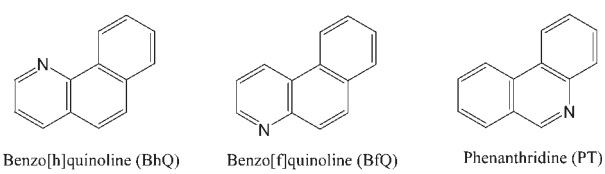

Benzo[h]quinoline (BhQ) Benzo[f]quinoline (BfQ) Phenanthridine (PT)

Scheme 1.

Published on the web July 4, 2006; doi:10.1246/bcsj.79.1039

Results and Discussion

pK_a and Apparent pK_a* Values of BhQ, BfQ, and PT. In neutral solutions, the absorption maxima of BhQ (1.7×10^{-4} mol dm^{-3}) were observed at 316, 330.5, and 346.5 nm. The absorption bands are due to a neutral species of BhQ, whose nitrogen atom is not protonated. The absorption maxima of BhQ in acidic solution were observed at 354.5 and 364 nm, with a shoulder at 310 nm. In the wavelength range examined, the absorption intensity in acidic solution was enhanced relative to that in neutral solution. The absorption bands of BhQ in acidic solution are due to a cationic species of BhQ, whose nitrogen atom is protonated. In acidic solutions, the fluorescence spectra of BhQ (3.7×10^{-5} mol dm^{-3}) showed a broad band peaked at about 435 nm, while in neutral solutions the fluorescence maxima were observed at 355, 372, and 389 nm.

From the absorbance change at 365 nm and the fluorescence intensity change at 370 nm, values of pK_a and apparent pK_a* for BhQ were evaluated to be 4.16 and 4.33, respectively. Similarly, pK_a and apparent pK_a* values of BfQ were estimated to be 4.92 and 5.05, respectively, and these values of PT were estimated to be 4.62 and 4.66, respectively. At pH 7.3, therefore, BhQ, BfQ, and PT exist as a neutral species in the ground and excited singlet states.

The pK_a and pK_a* values of BfQ are about 0.7 larger than those for BhQ, indicating that the basicity of BfQ is higher than that of BhQ. The Mulliken charges of the nitrogen atoms in BhQ and BfQ have been estimated to be -0.0838 and -0.19168, respectively. This is consistent with the experimental result that the pK_a value of BfQ is larger than those of BhQ. The pK_a and pK_a* values of PT are intermediates between those of BhQ and BfQ. The Mulliken charge (-0.07517) of a nitrogen atom in PT is larger than that for BhQ. However, the pK_a value of PT is larger than that of BhQ. This is probably because in the protonation and deprotonation, the nitrogen atom of BhQ is sterically hindered by a hydrogen atom of BhQ.

Inclusion Interactions of α- and β-CD with BhQ, BfQ, and PT. Interactions of α-CD with BhQ, BfQ, and PT: Addition of α-CD to pH 7.3 buffers of BhQ, BfQ, and PT resulted in little or no change in the absorption spectra of BhQ, BfQ, and PT. This indicates little or no formation of inclusion complexes of α-CD with BhQ, BfQ, and PT.

Absorption and Fluorescence Spectra of BhQ in Aqueous Solutions Containing β-CD: Figure 1 illustrates the absorption spectra of BhQ (1.7×10^{-4} mol dm^{-3}) in pH 7.3 buffers containing various concentrations of β-CD. Upon the addition of β-CD, the absorption maxima are shifted to shorter wavelengths, accompanied by an appearance of isosbestic points at 304, 328, 344, and 345 nm. In the presence of β-CD, the absorption bands are sharpened. The sharpening of the absorption bands suggests that, in β-CD solution, a BhQ molecule is in a relatively hydrophobic environment. These absorption spectral changes indicate the formation of an inclusion complex of β-CD with BhQ.

Figure 2 depicts the fluorescence spectra of BhQ (3.7×10^{-5} mol dm^{-3}) in pH 7.3 buffers containing various β-CD concentrations. As the β-CD concentration is increased, the

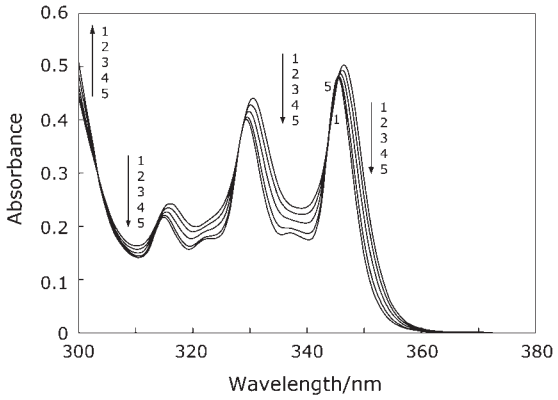

Fig. 1. Absorption spectra of BhQ (1.7×10^{-4} mol dm^{-3}) in pH 7.3 buffers containing various concentrations of β-CD. Concentration of β-CD: (1) 0, (2) 3.0×10^{-4}, (3) 1.0×10^{-3}, (4) 3.0×10^{-3}, and (5) 1.0×10^{-2} mol dm^{-3}.

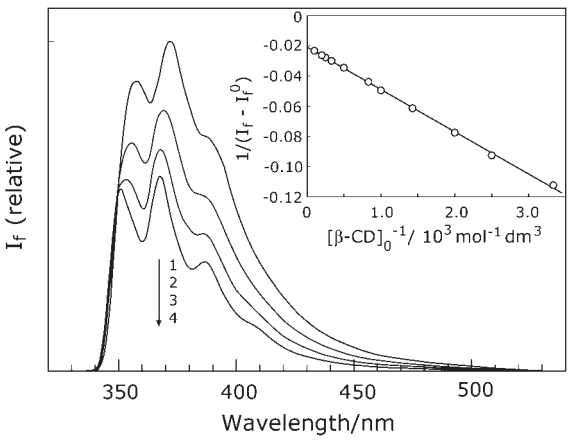

Fig. 2. Fluorescence spectra of BhQ (3.7×10^{-5} mol dm^{-3}) in pH 7.3 buffers containing various concentrations of β-CD. Concentration of β-CD: (1) 0, (2) 1.0×10^{-3}, (3) 3.0×10^{-3}, and (4) 1.0×10^{-2} mol dm^{-3}. $\lambda_{ex} = 328$ nm. Inset: Double reciprocal plot for the fluorescence intensity of BhQ (3.7×10^{-5} mol dm^{-3}) in pH 7.3 buffers containing β-CD. $\lambda_{ex} = 328$ nm. $\lambda_{obs} = 369$ nm.

BhQ fluorescence is decreased in intensity, accompanied by the shift of the fluorescence maxima to shorter wavelengths. The fluorescence bands are sharpened in the presence of β-CD. These fluorescence spectral changes as well as the absorption spectral changes indicate the formation of the inclusion complex of β-CD with BhQ.

When the 1:1 inclusion complex is formed between β-CD and BhQ, a double reciprocal relationship holds for the fluorescence intensity and the β-CD concentration:[2,15]

$$1/(I_f - I_f^0) = 1/a + 1/(aK_1[\beta\text{-CD}]_0). \quad (1)$$

Here, I_f, I_f^0, a, K_1, and $[\beta\text{-CD}]_0$ are the fluorescence intensity in the presence of β-CD, the fluorescence intensity in the absence of β-CD, a constant, the equilibrium constant for the formation of the 1:1 β-CD–BhQ inclusion complex, and the initial concentration of β-CD, respectively. The inset in Fig. 2 shows a plot of $1/(I_f - I_f^0)$ for BhQ against $1/[\beta\text{-CD}]_0$. The good linearity of the plot indicates the formation of the 1:1

Table 1. Values of K_1, K_2, and K_3 for BhQ, BfQ, and PT

	K_1/mol^{-1} dm^3		K_2/mol^{-1} dm^3		K_3/mol^{-1} dm^3
	β-CD	γ-CD	PO	THF	γ-CD
BhQ	750 ± 20	—	24.6	78.4	—
BfQ	490 ± 10	250 ± 30	10.3	37.1	2.18×10^5
PT	370 ± 10	150 ± 30	62.7	68.3	—

inclusion complex. From this plot, a K_1 value for BhQ is evaluated to be $750 \pm 20\,\mathrm{mol^{-1}\,dm^3}$ (Table 1). This K_1 value is half of the reported K_1 value ($1500 \pm 300\,\mathrm{mol^{-1}\,dm^3}$) for phenanthrene.[16] The small K_1 value for BhQ suggests that the hydrophobicity of BhQ is weaker than that of phenanthrene owing to the substitution of a nitrogen atom for a carbon atom.

Absorption and Fluorescence Spectra of BfQ in Aqueous Solutions Containing β-CD: When β-CD was added to BfQ ($1.6 \times 10^{-4}\,\mathrm{mol\,dm^{-3}}$) solution (pH 7.3), the absorption maxima of BfQ were slightly shifted to longer wavelengths, accompanied by the appearance of isosbestic points at 307, 333, and 346 nm (Fig. S1). The absorption spectral change indicates the formation of an inclusion complex between β-CD and BfQ. Upon the addition of β-CD to BfQ (6.5×10^{-5} $\mathrm{mol\,dm^{-3}}$) solution, the fluorescence bands were sharpened, the fluorescence intensity at longer wavelengths being considerably reduced (Fig. S2). The sharpening of the fluorescence bands in the presence of β-CD is consistent with the formation of the β-CD–BfQ inclusion complex, because the interior of the β-CD cavity is hydrophobic. From the fluorescence intensity change by the addition of β-CD, a K_1 value of BfQ has been evaluated to be $490 \pm 10\,\mathrm{mol^{-1}\,dm^3}$ (Table 1). The K_1 value for BfQ is smaller than that for BhQ, suggesting that the position of a nitrogen atom in a phenanthrene skeleton affects the binding ability towards the β-CD cavity. In BhQ and BfQ, the pyridine moiety fused to the naphthalene ring is less hydrophobic than the naphthalene ring. Consequently, the pyridine moiety most likely protrudes to the water environment, while the naphthalene ring is likely incorporated into the β-CD cavity from the secondary hydroxy-group side of β-CD.

Absorption and Fluorescence Spectra of PT in Aqueous Solutions Containing β-CD: As the β-CD concentration was increased, the absorption intensity of PT (9.9×10^{-5} $\mathrm{mol\,dm^{-3}}$) was reduced, accompanied by a shift of the absorption maxima to longer wavelengths (Fig. S3). Isosbestic points were observed at 318, 334, and 347.5 nm. These findings indicate the formation of an inclusion complex between β-CD and PT. In the presence of β-CD, the fluorescence intensity of PT in pH 7.3 buffer was decreased. The fluorescence spectral change of PT by the addition of β-CD was similar to that of BhQ, although the extent of the sharpening of the fluorescence band for PT was less than that for BhQ. The fluorescence spectral change also indicated the formation of the β-CD–PT inclusion complex. From a plot based on Eq. 1, a K_1 value of PT for β-CD was estimated to be $370 \pm 10\,\mathrm{mol^{-1}\,dm^3}$ (Table 1). The good linearity in the plot indicated the formation of the 1:1 β-CD–PT inclusion complex. The K_1 value of PT is the smallest among the three benzoquinolines examined. In contrast to BhQ and BfQ, PT does not have a hydrophobic naphthalene moiety, resulting in the smallest K_1 value.

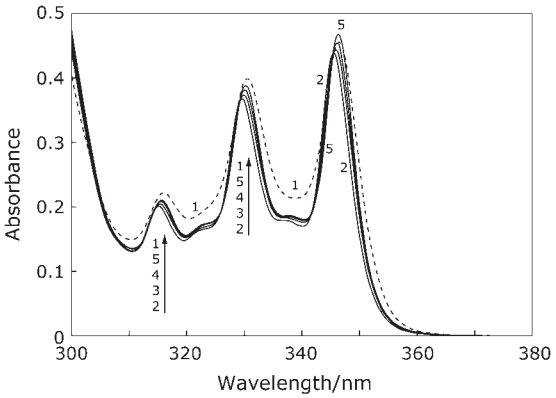

Fig. 3. Absorption spectra of BhQ ($1.5 \times 10^{-4}\,\mathrm{mol\,dm^{-3}}$) in pH 7.3 buffers containing β-CD ($3.0 \times 10^{-3}\,\mathrm{mol\,dm^{-3}}$) and various concentrations of PO. For spectrum 1, the β-CD and PO concentrations are zero. Concentration of PO: (1) 0, (2) 0, (3) 4.44×10^{-2}, (4) 7.40×10^{-2}, and (5) $1.48 \times 10^{-1}\,\mathrm{mol\,dm^{-3}}$.

Interactions of β-CD with BhQ, BfQ, and PT in Aqueous Solutions Containing Propylene Oxide (PO) or THF. Ternary Inclusion Complexes of BhQ: In the cases of aromatic compounds such as azulene, a ternary inclusion complex is formed among β-CD, an aromatic compound, and alcohol.[8,17,18] For heterocyclic compounds such as acridine and 2-methylnaphth[2,3-*d*]oxazole, the formation of the ternary inclusion complex of β-CD with alcohols has also been reported.[10,19] The addition of a small amount of 1-pentanol to BhQ solution containing β-CD resulted in little or no effect on the BhQ absorption spectrum. This finding suggests that BhQ does not form a ternary inclusion complex with β-CD and an alcohol molecule such as 1-pentanol. The vacant space within the β-CD cavity, which is occupied by a BhQ molecule, is likely shallow. Consequently, a 1-pentanol molecule, which is long in shape, may not be bound to the β-CD cavity including a BhQ molecule. Thus, we have tried to use PO, which is close to a sphere in shape compared to 1-pentanol. When PO is added to BhQ solution containing β-CD ($3.0 \times 10^{-3}\,\mathrm{mol\,dm^{-3}}$), the absorption bands of BhQ are shifted to longer wavelengths, accompanied by a sharpening of the absorption bands (Fig. 3). This absorption spectral change at the peaks is similar to that shown in Fig. 1, in which the β-CD concentration is varied in the absence of PO. In Fig. 3, however, the absorption band at the trough is changed little with the increase in the PO concentration. These findings suggest that the absorption spectral changes in Fig. 3 cannot be explained in terms of the apparent concentration variation of β-CD. Consequently, the absorption spectral change by the addition of PO is due to the formation of a ternary inclusion complex among β-CD, BhQ, and PO. Upon the addition of PO to BhQ solution containing β-CD, the fluorescence intensity of BhQ was enhanced with a sharpening of the fluorescence bands. The fluorescence spectral changes as well as the absorption spectral changes in the presence of PO indicate the formation of the ternary inclusion complex of β-CD, BhQ, and PO. Taking into account no formation of a ternary inclusion complex with 1-pentanol, a single PO molecule is most likely incorporated into the β-CD cavity bound to a BhQ molecule.

$$\beta\text{-CD}\cdot\text{BhQ} + \text{PO} \overset{K_2}{\rightleftharpoons} \beta\text{-CD}\cdot\text{BhQ}\cdot\text{PO}. \quad (2)$$

Here, K_2 is the equilibrium constant for the formation of the 1:1:1 β-CD–BhQ–PO inclusion complex (β-CD·BhQ·PO), and β-CD·BhQ is the 1:1 β-CD–BhQ inclusion complex. The fluorescence intensity, I_f, for BhQ solution containing both β-CD and PO is represented by

$$I_f = b[\text{BhQ}] + c[\beta\text{-CD}\cdot\text{BhQ}] + d[\beta\text{-CD}\cdot\text{BhQ}\cdot\text{PO}], \quad (3)$$

where b, c, and d are experimental constants including the fluorescence quantum yields of BhQ, β-CD·BhQ, and β-CD·BhQ·PO, respectively. Using the equilibrium constants, Eq. 3 is rewritten as

$$I_f = (b + cK_1[\beta\text{-CD}] + dK_1K_2[\beta\text{-CD}][\text{PO}])[\text{BhQ}]_0 / (1 + K_1[\beta\text{-CD}] + K_1K_2[\beta\text{-CD}][\text{PO}]), \quad (4)$$

where $[\text{BhQ}]_0$ is the initial concentration of BhQ. Figure 4 exhibits the least-squares best fit simulation curve for the BhQ fluorescence intensity as a function of the PO concentration. In the simulation, the already evaluated K_1 value (750 $\text{mol}^{-1}\,\text{dm}^3$) has been used, and values of K_2, b, c, and d have been assumed to be 24.6, 1.76×10^6, 2.51×10^6, and $2.81 \times 10^6\,\text{mol}^{-1}\,\text{dm}^3$, respectively.

The addition of THF to BhQ solution containing β-CD also resulted in absorption and fluorescence spectral changes similar to those for PO. Consequently, the ternary inclusion complex is also formed among β-CD, BhQ, and THF. A simulation similar to that used for PO gave $78.4\,\text{mol}^{-1}\,\text{dm}^3$ as a K_2 value of THF, which is about three times greater than that for PO (Table 1). This suggests that a THF molecule is more appropriate in size than a PO molecule for the invasion to the vacant space inside the β-CD cavity in the 1:1 β-CD–BhQ inclusion complex.

Ternary Inclusion Complexes of BfQ and PT: When PO (or THF) was added, absorption spectral changes similar to that for BhQ were observed for BfQ and PT in β-CD solution.

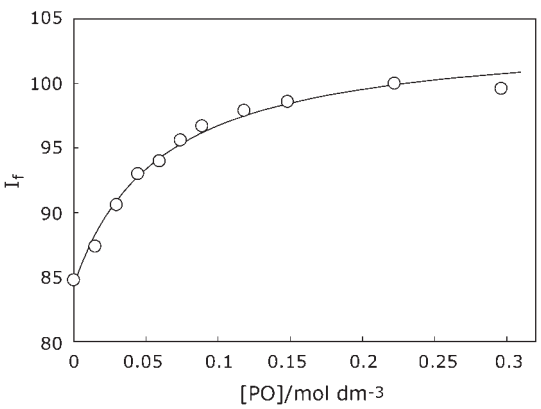

Fig. 4. Simulation of the observed fluorescence intensities in BhQ solution containing β-CD and PO. The best fit simulation curve for the 1:1:1 β-CD–BhQ–PO inclusion complex has been calculated with the evaluated K_1 value of $750\,\text{mol}^{-1}\,\text{dm}^3$, under the assumptions of $b = 1.76 \times 10^6$, $c = 2.51 \times 10^6$, $d = 2.81 \times 10^6$, and $K_2 = 24.6\,\text{mol}^{-1}\,\text{dm}^3$. $[\text{BhQ}]_0 = 3.7 \times 10^{-5}\,\text{mol}\,\text{dm}^{-3}$. $[\beta\text{-CD}]_0 = 3.0 \times 10^{-3}\,\text{mol}\,\text{dm}^{-3}$. $\lambda_{ex} = 328\,\text{nm}$. $\lambda_{obs} = 352\,\text{nm}$.

The absorption spectral changes suggest the formation of ternary inclusion complexes of β-CD–BfQ–PO (or THF) and β-CD–PT–PO (or THF). With an increase in the PO (or THF) concentration, the fluorescence intensity of BfQ in β-CD solution was reduced, accompanied by a sharpening of the fluorescence bands. In contrast, the fluorescence intensity of PT in β-CD solution was enhanced by the addition of PO (or THF). The fluorescence spectral changes indicate the formation of the ternary inclusion complexes of β-CD–BfQ–PO (or THF) and β-CD–PT–PO (or THF). Using a simulation method similar to that used for BhQ, K_2 values of BfQ were estimated to be 10.3 and $37.1\,\text{mol}^{-1}\,\text{dm}^3$ for PO and THF, respectively (Table 1). These K_2 values for BfQ are about half of the K_2 values for BhQ, respectively.

Similarly, the K_2 values for PT were evaluated to be 62.7 and $68.3\,\text{mol}^{-1}\,\text{dm}^3$, respectively (Table 1). The K_2 values of PT for PO and THF are greater than those of BfQ for PO and THF, respectively. The K_2 value of PT for PO is also greater than that of BhQ for PO, although the K_2 value of PT for THF is less than that of BhQ for THF. The reason for the large K_2 values for PT is not clear at present. For BhQ and BfQ, the K_2 value for THF is about three times greater than that for PO. In the case of PT, on the other hand, the K_2 value for THF is slightly greater than that for PO. Consequently, another factor besides the free volume within the β-CD cavity of the binary inclusion complexes, which is not clear at present, may affect the magnitude of the K_2 value for PT.

Inclusion Interactions of γ-CD with BhQ, BfQ, and PT. Absorption and Fluorescence Spectra of BfQ in Aqueous Solution Containing γ-CD: Upon the addition of γ-CD, a BhQ solution (pH 7.3) turned turbid even at low BhQ concentrations. Consequently, we did not further examine the interactions between γ-CD and BhQ.

Figure 5 exhibits absorption spectra of BfQ ($1.6 \times 10^{-4}\,\text{mol}\,\text{dm}^{-3}$) in pH 7.3 buffers containing various concentrations of γ-CD. When γ-CD is added, the absorption maxima are very slightly shifted to longer wavelengths, accompanied by an appearance of isosbestic points at 312, 334, 337, and 348.5 nm. This finding suggests the formation of an inclusion complex of γ-CD with BfQ. Upon the addition of γ-CD to BfQ ($6.5 \times 10^{-5}\,\text{mol}\,\text{dm}^{-3}$) solution, the fluorescence band

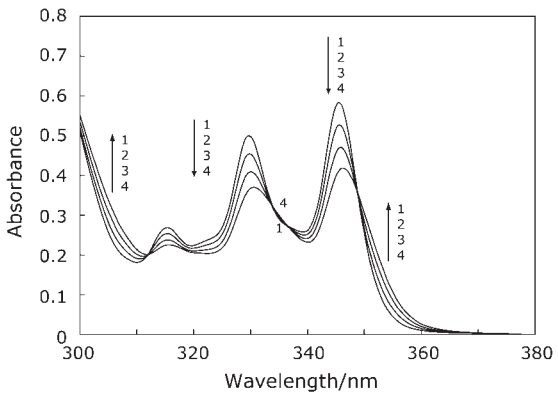

Fig. 5. Absorption spectra of BfQ ($1.6 \times 10^{-4}\,\text{mol}\,\text{dm}^{-3}$) in pH 7.3 buffers containing various concentrations of γ-CD. Concentration of γ-CD: (1) 0, (2) 3.0×10^{-4}, (3) 1.0×10^{-3}, and (4) $3.0 \times 10^{-3}\,\text{mol}\,\text{dm}^{-3}$.

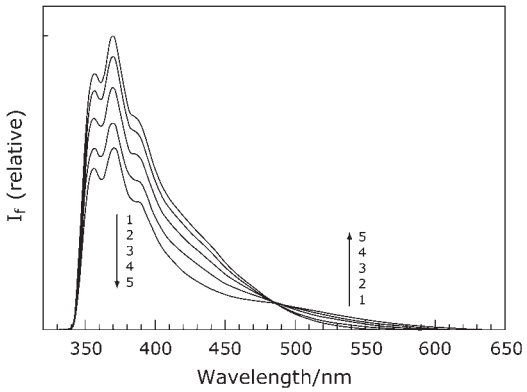

Fig. 6. Fluorescence spectra of BfQ (6.5×10^{-5} mol dm^{-3}) in pH 7.3 buffers containing various concentrations of γ-CD. Concentration of γ-CD: (1) 0, (2) 3.0×10^{-4}, (3) 1.0×10^{-3}, (4) 3.0×10^{-3}, and (5) 1.0×10^{-2} mol dm^{-3}. $\lambda_{ex} = 333$ nm.

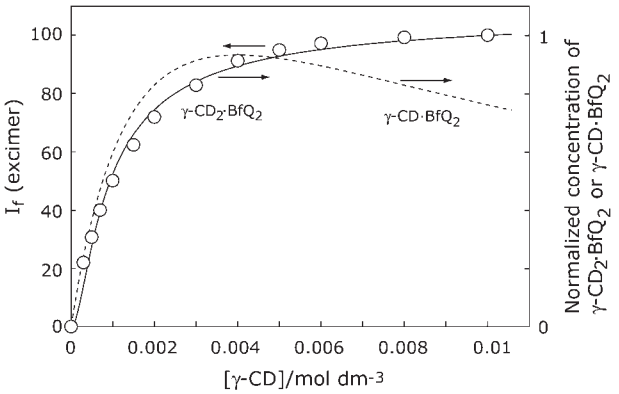

Fig. 7. Simulation of the observed excimer fluorescence intensities of BfQ. The best fit simulation curve (solid line) for the 2:2 γ-CD–BfQ inclusion complex has been calculated with the evaluated K_1 value of 250 mol^{-1} dm^3 and an assumed K_3 value of 2.18×10^5 mol^{-1} dm^3. The best fit simulation curve (dotted line) for the 1:2 γ-CD–BfQ inclusion complex has been calculated with the evaluated K_1 value of 250 mol^{-1} dm^3 and an assumed K_3' value of 2.55 mol^{-1} dm^3. $[BfQ]_0 = 6.5 \times 10^{-5}$ mol dm^{-3}. $\lambda_{ex} = 333$ nm. $\lambda_{obs} = 530$ nm.

at 370 nm is reduced in intensity, accompanied by an increase in the intensity of the longer-wavelength band tail (Fig. 6). At a low concentration (6.5×10^{-6} mol dm^{-3}) of BfQ, the longer-wavelength band did not appear in the presence of γ-CD. Consequently, the longer-wavelength band is due to the excimer fluorescence of BfQ. Because there are isosbestic points in the absorption spectra, the absorption spectrum of the species emitting excimer fluorescence is very similar to that of the 1:1 γ-CD–BfQ inclusion complex. Alternatively, the concentration of the species emitting the excimer fluorescence is low compared to the concentration of the 1:1 inclusion complex.

Although the 2:2 γ-CD–guest inclusion complexes responsible for the excimer fluorescence have been known for pyrene, sodium 1-pyrenebutyrate, 2-methylnaphthalene, and so on, the 1:2 γ-CD–guest inclusion complexes have also been reported for Methyl Orange, Methylene Blue, thionine, Pyronine Y, and others.[20–28] The excimer fluorescence may be due to the 2:2 γ-CD–BfQ inclusion complex (γ-CD_2·BfQ_2) or the 1:2 γ-CD–BfQ inclusion complex (γ-CD·BfQ_2):

$$\gamma\text{-CD}\cdot\text{BfQ} + \gamma\text{-CD}\cdot\text{BfQ} \overset{K_3}{\rightleftharpoons} \gamma\text{-CD}_2\cdot\text{BfQ}_2, \quad (5)$$

or

$$\gamma\text{-CD}\cdot\text{BfQ} + \text{BfQ} \overset{K_3'}{\rightleftharpoons} \gamma\text{-CD}\cdot\text{BfQ}_2. \quad (6)$$

Here, K_3 is the equilibrium constant for the formation of the 2:2 γ-CD–BfQ inclusion complex, γ-CD·BfQ stands for the 1:1 γ-CD–BfQ inclusion complex, and K_3' is the equilibrium constant for the formation of the 1:2 γ-CD–BfQ inclusion complex. To identify the inclusion complex responsible for the excimer fluorescence, we first evaluated a K_1 value of BfQ for γ-CD. As previously stated, the addition of γ-CD to a dilute BfQ solution such as 6.5×10^{-6} mol dm^{-3} did not cause the intensity enhancement in the longer-wavelength tail. In the dilute BfQ solution, therefore, a 1:1 γ-CD–BfQ inclusion complex alone is formed. From the fluorescence intensity change by the addition of γ-CD to dilute BfQ solution, a K_1 value for γ-CD has been estimated to be 250 ± 30 mol^{-1} dm^3 (Table 1). This K_1 value is about half of that for β-CD, suggesting that the larger γ-CD cavity does not fit the size of the BfQ molecule as much as the β-CD cavity does.

Under our experimental conditions, the excimer fluorescence intensity is proportional to the concentration of the species emitting the excimer fluorescence. When the excimer fluorescence is due to the 2:2 inclusion complex, the excimer fluorescence intensity I_f^{ex} is represented by

$$I_f^{ex} = e[\gamma\text{-CD}_2\cdot\text{BfQ}_2]. \quad (7)$$

Here, e is an experimental constant including the fluorescence quantum yield of the 2:2 γ-CD–BfQ inclusion complex. Using the equilibrium constants, Eq. 7 is rewritten as

$$I_f^{ex} = eK_1^2K_3[\gamma\text{-CD}]^2[\text{BfQ}]^2. \quad (8)$$

The initial concentration of BfQ, $[BfQ]_0$, is given by

$$[\text{BfQ}]_0 = [\text{BfQ}] + [\gamma\text{-CD}\cdot\text{BfQ}] + 2[\gamma\text{-CD}_2\cdot\text{BfQ}_2]. \quad (9)$$

By the use of the equilibrium constants, we obtain a quadratic equation for [BfQ] from Eq. 9:

$$2K_1^2K_3[\gamma\text{-CD}]^2[\text{BfQ}]^2 + (1 + K_1[\gamma\text{-CD}])[\text{BfQ}] - [\text{BfQ}]_0 = 0. \quad (10)$$

Using an assumed K_3 value and the evaluated K_1 value (250 mol^{-1} dm^3), [BfQ] can be calculated from Eq. 10. Consequently, the excimer fluorescence intensity at a given γ-CD concentration can be evaluated from Eq. 8 under the assumed values of e and K_3. The result of the simulation for the excimer fluorescence intensity is shown in Fig. 7. The least-squares best fit simulation curve, which has been calculated using an assumed value of K_3 (2.18×10^5 mol^{-1} dm^3 (Table 1)), fits the observed excimer fluorescence data well. The good fit in the simulation indicates that the excimer fluorescence is due to the 2:2 γ-CD–BfQ inclusion complex.

For the evaluation of the initial concentration of BfQ used in the simulation, the molar absorption coefficients in water and

methanol have been assumed to be the same. The shape of the simulation curve and the K_3 value are dependent on the initial concentration of BfQ (Eqs. 8 and 10). Thus, we examined the influence of the initial concentration of BfQ on the shape of the simulation curve and the K_3 value. The simulation was made for the concentration of the 2:2 γ-CD–BfQ inclusion complex using the initial concentrations of BfQ, which were respectively 20% higher (7.8×10^{-5} mol dm^{-3}) and 20% lower (5.2×10^{-5} mol dm^{-3}) than the initial concentration (6.5×10^{-5} mol dm^{-3}) estimated from the molar absorption coefficient in methanol. Even when the 20% higher or 20% lower concentration of BfQ was employed for the calculation of the simulation curve, it fitted the excimer fluorescence intensity data well, indicating that the 2:2 γ-CD–BfQ inclusion complex is responsible for the excimer fluorescence. The error of 20% for the BfQ concentration hardly affected the shape of the simulation curve. From the simulation, the K_3 values for the 20% higher and 20% lower initial concentrations of BfQ were estimated to be 1.84×10^5 and 2.74×10^5 mol^{-1} dm^3, respectively. These K_3 values are respectively about 16% smaller and about 25% larger than the K_3 value estimated using the molar absorption coefficient in methanol. Furthermore, we performed the simulation for the 2:2 inclusion complex in which the 50% higher and 50% lower initial concentrations of BfQ were used. The simulation curves thus obtained also fitted the observed fluorescence data well.

To further confirm the origin of the BfQ excimer fluorescence, we performed a simulation based on the other scheme (Eq. 6), in which the 1:2 γ-CD–BfQ inclusion complex is responsible for the excimer fluorescence. In this scheme, the excimer fluorescence intensity is given by

$$I_f^{ex} = fK_1K_3'[\gamma\text{-CD}][\text{BfQ}]^2, \tag{11}$$

where f is an experimental constant including the fluorescence quantum yield of the 1:2 γ-CD–BfQ inclusion complex. The BfQ concentration can be calculated by solving the equation:

$$2K_1K_3'[\gamma\text{-CD}][\text{BfQ}]^2 + (1 + K_1[\gamma\text{-CD}])[\text{BfQ}] - [\text{BfQ}]_0 = 0. \tag{12}$$

The best fit simulation curve thus obtained for the 1:2 γ-CD–BfQ inclusion complex is also shown in Fig. 7. In contrast to the best fit simulation curve for the 2:2 γ-CD–BfQ inclusion complex, the best fit simulation curve for the 1:2 inclusion complex does not reproduce the observed excimer fluorescence intensities. This result supports that the excimer fluorescence is due to the 2:2 γ-CD–BfQ inclusion complex. As in the case of the simulation for the formation of the 2:2 γ-CD–BfQ inclusion complex, the best fit simulation curves for the 1:2 γ-CD–BfQ inclusion complex were calculated under the conditions that the 20% higher and 20% lower initial concentrations of BfQ were used. However, these simulation curves did not fit the observed fluorescence intensity data. This finding indicates that the error of 20% for the initial concentration of BfQ hardly affects the shape of the simulation curve for the 1:2 γ-CD–BfQ inclusion complex.

Because the inner space of the two γ-CD cavities in the 2:2 γ-CD–BfQ inclusion complex is not so wide, the two BfQ rings seem to partially overlap upon the formation of the excimer.

K_3 values of the 1:1 β-CD–naphthalene derivative inclusion complexes have been reported to be 1400, 3370, 4000, 5830, 48400, and 70000 mol^{-1} dm^3, for 2-methylnaphthalene, 2-ethylnaphthalene, naphthalene, 1-methylnaphthalene, 1-chloronaphthalene, and 1-cyanonaphthalene, respectively.[2,18,24,29,30] On the other hand, K_3 values of the 1:1 γ-CD–2-methylnaphthalene and γ-CD–1-chloronaphthalene inclusion complexes are 3.38×10^6 and 2.16×10^7 mol^{-1} dm^3, respectively.[24,31] As with the above naphthalene derivatives, therefore, the K_3 values for γ-CD are greater than those for β-CD. The K_3 value of 2.18×10^5 mol^{-1} dm^3 for BfQ is greater than that of β-CD for the naphthalene derivatives, but one to two orders of magnitude less than those of γ-CD for the naphthalene derivatives.

Absorption and Fluorescence Spectra of PT in Aqueous Solution Containing γ-CD: At high PT concentrations such as 9.9×10^{-5} mol dm^{-3}, the addition of γ-CD resulted in a slightly turbid solution. To avoid the turbidity of the PT solution, therefore, a low concentration of PT was employed for the addition of γ-CD. For the dilute PT solution (3.3×10^{-5} mol dm^{-3}), an absorption spectral change similar to that for β-CD was observed upon the addition of γ-CD. This finding suggests the formation of a γ-CD–PT inclusion complex. At a PT concentration of 3.3×10^{-5} mol dm^{-3}, the fluorescence intensity of PT was decreased by the addition of γ-CD, without enhancement of the intensity of the longer-wavelength band tail. This fluorescence spectral change for γ-CD is similar to that for β-CD. Combined with no observation of the PT excimer fluorescence, the decrease in the fluorescence intensity suggests the formation of the 1:1 γ-CD–PT inclusion complex. From a plot based on Eq. 1, a K_1 value of PT for γ-CD was evaluated to be 150 ± 30 mol^{-1} dm^3 (Table 1). The K_1 value for PT is 60% of that for BfQ. The small K_1 value of γ-CD for PT is parallel to the result that the K_1 value of β-CD for PT is less than that for BfQ. As previously stated, the absence of a naphthalene moiety in PT is likely responsible for the K_1 values of PT for β- and γ-CD being less than those of BfQ and responsible for the K_1 value of PT for β-CD being less than that of BhQ for β-CD.

Conclusion

The interactions of the benzoquinolines (BhQ, BfQ, and PT) with α-, β-, and γ-CDs have been examined in pH 7.3 buffers, in which the benzoquinolines exist as a neutral species in the ground and excited singlet states. Little or no interactions between the benzoquinolines and α-CD have been observed. The neutral species of the benzoquinolines form inclusion complexes with β-CD; the 1:1 inclusion complexes are formed. In addition, BfQ and PT form the 1:1 inclusion complex with γ-CD. For BfQ, the 2:2 γ-CD–BfQ inclusion complex, which is responsible for the BfQ excimer fluorescence, is also formed. The K_1 values of PT for β- and γ-CD are less than those of BfQ for β- and γ-CD, respectively. Furthermore, the K_1 value of PT for β-CD is less than that of BhQ for β-CD. These findings indicate that the position of a nitrogen atom substituted in the phenanthrene ring affects the inclusion interactions with CDs. The ternary inclusion complexes of BhQ, BfQ, and PT with β-CD and PO (or THF) are formed. The K_2 values of BfQ for PO and THF are less than those of BhQ and PT.

Supporting Information

Figures S1–S3 in PDF format. This material is available free of charge on the web at: http://www.csj.jp/journals/bcsj/.

References

1 K. Kano, I. Takenoshita, T. Ogawa, *Chem. Lett.* **1982**, 321.
2 S. Hamai, *Bull. Chem. Soc. Jpn.* **1982**, *55*, 2721.
3 G. Patonay, K. Fowler, A. Shapira, G. Nelson, I. M. Warner, *J. Inclusion Phenom.* **1987**, *5*, 717.
4 S. Hamai, *J. Phys. Chem.* **1989**, *93*, 6527.
5 S. Hamai, *J. Phys. Chem.* **1989**, *93*, 2074.
6 S. Hamai, *J. Am. Chem. Soc.* **1989**, *111*, 3954.
7 A. Munoz de la Pena, T. T. Ndou, J. B. Zung, K. L. Greene, D. H. Live, I. M. Warner, *J. Am. Chem. Soc.* **1991**, *113*, 1572.
8 S. Hamai, T. Ikeda, A. Nakamura, H. Ikeda, A. Ueno, F. Toda, *J. Am. Chem. Soc.* **1992**, *114*, 6012.
9 J. M. Schuette, T. Ndou, A. Munoz de la Pena, K. L. Greene, C. K. Williamson, I. M. Warner, *J. Phys. Chem.* **1991**, *95*, 4897.
10 J. M. Schuette, T. T. Ndou, A. Munoz de la Pena, S. Mukundan, Jr., I. M. Warner, *J. Am. Chem. Soc.* **1993**, *115*, 292.
11 X. Shen, M. Belletete, G. Durocher, *Langmuir* **1997**, *13*, 5830.
12 M. Maafi, J. Aaron, M. C. Mahedero, F. Salinas, *Appl. Spectrosc.* **1998**, *52*, 91.
13 J. Dey, E. L. Roberts, I. M. Warner, *J. Phys. Chem. A* **1998**, *102*, 301.
14 P. Rodriguez, M. Sanchez, J. R. Isasi, G. Gonzalez-Gaitano, *Appl. Spectrosc.* **2002**, *56*, 1490.
15 H. A. Benesi, J. H. Hildebrand, *J. Am. Chem. Soc.* **1949**, *71*, 2703.
16 I. Sanemasa, T. Takuma, T. Deguchi, *Bull. Chem. Soc. Jpn.* **1989**, *62*, 3098.
17 S. Hamai, *Bull. Chem. Soc. Jpn.* **1989**, *62*, 2763.
18 S. Hamai, *J. Phys. Chem.* **1990**, *94*, 2595.
19 S. Hamai, *Bull. Chem. Soc. Jpn.* **2004**, *77*, 1459.
20 N. Kobayashi, R. Saito, H. Hino, Y. Hino, A. Ueno, T. Osa, *J. Chem. Soc., Perkin Trans. 2* **1983**, 1453.
21 S. Hamai, *J. Phys. Chem.* **1989**, *93*, 6527.
22 W. G. Herkstroeter, P. A. Martic, S. Farid, *J. Chem. Soc., Perkin Trans. 2* **1984**, 1453.
23 W. G. Herkstroeter, P. A. Martic, T. R. Evans, S. Farid, *J. Am. Chem. Soc.* **1986**, *108*, 3275.
24 S. Hamai, *Bull. Chem. Soc. Jpn.* **1996**, *69*, 543.
25 H. Hirai, N. Toshima, S. Uenoyama, *Bull. Chem. Soc. Jpn.* **1985**, *58*, 1156.
26 S. Hamai, H. Satou, *Bull. Chem. Soc. Jpn.* **2000**, *73*, 2207.
27 S. Hamai, *Bull. Chem. Soc. Jpn.* **2000**, *73*, 861.
28 R. L. Schiller, S. F. Lincoln, J. H. Coates, *J. Chem. Soc., Faraday Trans. 1* **1987**, *83*, 3237.
29 S. Hamai, A. Hatamiya, *Bull. Chem. Soc. Jpn.* **1996**, *69*, 2469.
30 S. Hamai, *J. Phys. Chem. B* **1999**, *103*, 293.
31 S. Hamai, *J. Mater. Chem.* **2005**, *15*, 2881.